Modelling of silver adhesion on MgO(100) surface with defects

Yu F Zhukovskii†‡, E A Kotomin†§¶, P W M Jacobs‡, A M Stoneham∥ and
J H Harding∥

† Institute of Solid State Physics, University of Latvia, Kengaraga 8, LV-1063 Riga, Latvia
‡ Department of Chemistry, University of Western Ontario, London, Ontario N6A 5B7, Canada
§ Max Planck Institut für Festkörperphysik, Heisenberg strasse 1, D-70569 Stuttgart, Germany
∥ Centre for Materials Research, Department of Physics and Astronomy,
University College London, Gower Street, London WC1E 6BT, UK

E-mail: kotomin@latnet.lv

Abstract.   We show how surface defects (especially F_s^0 and V_s^0 centres) can play a major role in
the adhesion of Ag (at 1:4 and 1:1 coverages) on the MgO(100) surface. Our calculations use a
periodic (slab) model and an *ab initio* Hartree–Fock approach with *a posteriori* electron correlation
corrections. We are able to analyse the interatomic bond populations, effective charges and
multipole moments of ions, in combination with the interface binding energy and the equilibrium
distances. Both surface defects cause strong redistributions of the electron density which increase
the binding energy of metal atoms by more than an order of magnitude. This implies radiation-
induced strengthening of metal adhesion on oxide substrates and clarifies defect mechanisms in
nucleating film growth. We compare our atomistic predictions with those from simpler methods
which might be used for complex technologically interesting systems. There is good general
agreement with the image interaction model; differences arise partly from different treatments of
dispersion and partly from subtle but significant charge redistribution in the Ag. Further, a simple
Born–Haber analysis of charge transfer is consistent with the several cases predicted in the atomistic
calculations.

1. Introduction

The control of metal/oxide interfaces in their many technological applications depends on the
quantitative understanding of adhesion and of the kinetics and mechanisms of metal film growth
on oxide surfaces (see [1–6] and references therein). This understanding contains significant
gaps, despite many theoretical studies, mostly of the adhesion of noble and transition metals on
MgO substrates [7–17]. Partly this is because of the very sensitive balance between the various
energy contributions. Perhaps the successes are more surprising than the inconsistencies. This
is especially true when the range of atomistic methods is noted. *Cluster* models [8, 9, 15] and
slab models (periodic in two dimensions) [11–14] have been applied to defect-free interfaces; a
few calculations have attempted proper *embedding* [18]. An *ab initio* Hartree–Fock formalism
has been used in cluster models of Me/MgO interfaces [8, 9]. For metal adhesion on MgO
surfaces, methods applied include the local density approximation (LDA) as a full-potential
linearized muffin-tin orbital method (FP LMTO) in a slab model [11, 12], full-potential
linearized augmented plane waves (FP LAPWs) [13] and self-consistent local orbitals (LOs)
[14, 15]. We have recently made Hartree–Fock calculations for the Ag/MgO(100) interface

¶ Corresponding author.

using a slab model [16]. The modelling of the complex, technological metal/oxide systems requires simpler methods. Examples are the image interaction model (IIM) (Stoneham and Tasker [2], [7]) and the shell model (SM; this model is also used in many IIM calculations) [17].

Tests of predictions come from several types of experiment. Results for atomic structure nowadays could be compared directly with high-resolution electron microscopy data, at least for a few metal/oxide (e.g. Ag/MgO) interfaces [25] at near-atomic resolution. For liquid metal/oxide interfaces, there are data for adhesion energies and wetting angles. Wetting (small wetting angle) often implies a chemical reaction between the liquid metal and the oxide substrate. For non-reactive liquid metals, there are systematic trends of wetting angle with substrate [7]. Yet there is significant adhesion even without reaction. For Ag/MgO, our calculations (both HF [16] and IIM [20]) showed negligible chemical reaction of Ag with perfect MgO surfaces. The major term in adhesion comes from polarization of the metal by the oxide ions (the major IIM mechanism), plus electronic density accumulation in gap positions between atoms in the metal film, as discovered in the HF calculations.

For thin solid metal films on oxides, what is seen depends strongly on growth conditions. Thus, Ag growth on MgO usually yields 3D islands [19, 21]. Yet a recent low-energy-electron-diffraction study showed a layer-by-layer growth mode could occur for silver deposited on vacuum-cleaved MgO(100) surfaces, even though the structure is metastable [22]. Partly, this is a matter of kinetics: the rate of Ag deposition, and competition between surface processes [23]. It is clear that defects can be critical in determining the growth mode, since metal clusters nucleate and grow mainly at defect sites [1]. Experiment shows defects on an MgO(100) surface serve as nuclei for the growth of metal clusters on oxide substrates [5, 24], a continuous metal film forming after clusters overlap. This agrees with calculations [10] showing a delicate energy balance between Ag island and monolayer-mode growth.

As first suggested by Stoneham and Tasker (1986) [25], *charged* (e.g. radiation-induced) defects increase the adhesion energy via the image interaction between charged oxide defects and the metal. Calculations [20] predict a maximum interaction between a vacancy in MgO and a metal of ≈ 2 eV per defect. Similar values were found in atomistic SM calculations for ten layers of Ag on an MgO(100) surface with O vacancies [15]. Our main concern here is with effects which go beyond these simpler yet useful approaches, so as to understand electron transfer and redistribution for metal atoms at defect sites on the oxide surface. We find our quantum calculations both support the earlier approaches and point to new and simple ideas which will make analysis of more complex systems practical.

Early HF cluster calculations [8] showed that Cu atoms bind strongly to Mg vacancies, each Cu atom donating two electrons to the surrounding O atoms to become a Cu^{2+} ion replacing a missing Mg^{2+} ion; the binding energy indicated was 9 eV per Cu atom. Later cluster calculations [9] also show electron redistibution between Rb, Pd and Ag atoms and surface F_s-type centres (surface O vacancy with 0, 1 or 2 electrons) and V_s-type centres (surface Mg vacancy with holes trapped on nearest O ions). However, the use of small and often strongly charged clusters in these calculations can lead to major errors in binding energies if polarization energies are not treated with care (Stoneham and Tasker 1985 [25]). Cluster HF calculations (Matveev *et al* [15]) predict an Ag atom binding energy of 0.02 eV, much smaller than we find in slab calculations. This is why we use here a periodic, infinite in two dimensions, slab model. We study the Ag/MgO(100) interface by a first-principles Hartree–Fock formalism. We demonstrate the special role of surface defects in the first stages of metal adhesion on MgO. Our results are compared with quantum mechanical cluster calculations and the phenomenological IIM and SM studies, and lead to a consistent picture of metal adhesion associated with oxide defects.

2. Theory

We use the *ab initio* Hartree–Fock code CRYSTAL95 for periodic systems [26], with electron correlation corrections (HF-CC method) calculated using density-functional theory [27]. Such terms are needed, as standard HF theory underestimates binding energies and overestimates molecular bond lengths. We use *a posteriori* corrections in the non-local Perdew–Wang generalized gradient approximation (PWGGA) [28]. The MgO basis set (BS), optimized previously [29], consists of all-electron 8-61G and 8-51G functions (s and sp shells) for Mg and O atoms, respectively. To reduce computation, we employed Hay–Wadt small-core (HWSC) pseudopotentials for Ag atoms [30], so reducing the total number of electrons per Ag to 19 ($4s^2 4p^6 4d^{10} 5s^1$). An initial guess for the valence BS of silver (311-31G for sp and d shells) was taken from AgCl calculations [31], and the outer exponents were re-optimized [16]. Calculations starting from the Ag $4d^9 5s^2$ configuration give essentially the same results. We have estimated *a posteriori* electron correlation corrections to the total energy in our HF calculations. They prove to be about 0.5% of the HF total energy, and are almost independent of interface distance.
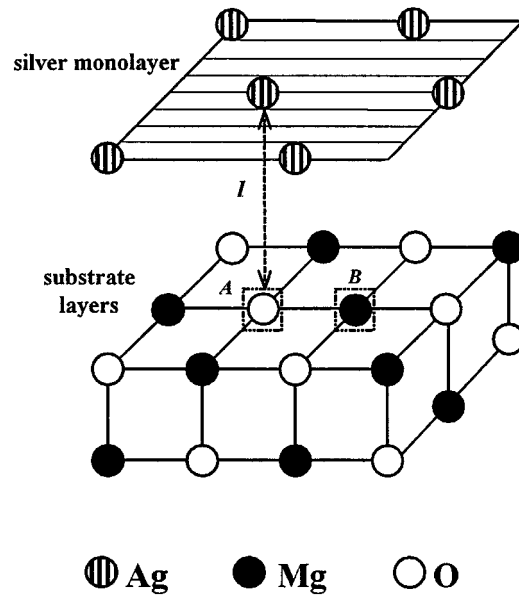

Figure 1. Sketch of Ag/MgO(100) interface, with Ag atoms placed at a distance l above either the surface F_s centres (A) (or O^{2-} ions on the perfect substrate), or above the V_s centres (B) (or the regular Mg^{2+} ions). The surface concentration of defects is 1:4.

The CRYSTAL95 code is well suited to treating finite-thickness slabs as two-dimensional periodic systems. We have simulated the Ag/MgO(100) interface with either a low surface coverage (1:4) by Ag atoms, (which models an early stage of metal film adhesion), and with one to three Ag layers atop three layers of the oxide substrate. The optimized value of the lattice constant for the three-layer MgO slab (4.21 Å [16]) is very close to the experimental bulk value (4.205 Å [29]). In line with all previous calculations, we ignore the small (3%) mismatch in the lattice constants of fcc Ag and MgO, although we recognize that we need to consider mismatch dislocations when we compare with experiment. In our calculations, we fix the lattice constant along the surface xy plane at 4.21 Å. We allow the interfacial (metal–substrate) distance to

vary along the z axis, perpendicular to the interface. The distances between different silver planes within the metal slab are also free to change.

For all perfect and defective configurations, the binding energy was calculated as difference of the two total energies, that for the interface with optimized geometry and that for the two separate slabs. To find the binding energy correctly, we calculated carefully the interface potential energy curve versus the interface distance. As the distance increased to large values, we used as an initial guess for SCF procedure the density matrix of the interface configuration with slightly closer separation. In this way, we could avoid the so-called 'polarization catastrophe' for widely separated slabs. If one calculates the binding energy for a defective interface using some of the traditional formulae, the interface energy inevitably includes an error.

Results in table 1 are for the most likely sites for Ag adsorption: above surface O^{2-} ions and above surface Mg^{2+} ions. Surface defects on the MgO substrate are modelled by removing one of four O or Mg atoms from the 2×2 extended surface unit cell (figure 1). By removing neutral atoms, we retain neutral supercells, with *neutral* surface F_s^0 centres, or V_s^0 centres. Charged defects are not discussed in this paper. We leave in the vacancy the basis set of the missing atom (the so-called *ghost* [26]); without this part of the basis set, we should have a poor representation of the neutral defect. Atomic relaxation of the MgO structure around these defects has been found for the isolated MgO slabs and reoptimized for the Ag/MgO interface with defects.

3. Results and discussion

3.1. Perfect interface

First, we consider the favoured adsorption site for Ag on the perfect MgO surface. For full (1:1) coverage, HF-CC predicts adsorption over the surface O atoms is favoured energetically. This agrees with recent experiments [32] and with three previous LDA-type calculations [11–13]. It contradicts those IIM results [18, 33] for which the most accurate treatment of the dispersion forces was included, but agrees with an *image model* (IM) approach which used a less accurate treatment of dispersion. The main difference from the IIM appears arise from the strength of the long-range dispersion forces between the Ag and the O neighbours of the Mg site below the Ag. Shell model calculations [17], broadly equivalent to the IIM, predict preferential adsorption over O^{2-}, with a low adhesion energy of only 0.11 eV. This value, smaller than our predictions, may result from neglect of the electron density redistribution within the metal plane. Our present results show that a large part of the differences in detail between full electronic structure calculations and these approaches stems from relatively subtle shifts in Ag charge density.

When Ag is above O, all microscopic methods give similar spacings between the outer MgO plane and the Ag which faces it, with values in a narrow range 2.4 to 2.7 Å. The image model result agrees (2.53 Å), as does the SM (2.60 Å). Our HF-CC value of 2.43 Å for three metal layers agrees with recent experimental data [32]. For a three-layer Ag film with Ag over O, the HF-CC adhesion energy of 0.46 eV is smaller than the value of 0.88 eV from FP LAPW calculations [11]; an even lower value is found for Ag over Mg by HF-CC (table 1). The relevant experimental estimate is 0.26 eV [19], which is probably lower than the value for a defect-free surface because of misfit dislocations arising from the 3% difference in lattice parameters of Ag and MgO.

There is negligible chemical bonding across a defect-free interface between metal and oxide substrate: *the adhesion is physical in origin, and mainly due to polarization of the*

metal by the ions. Calculated Mulliken charges on Ag atoms ($e(00)$ column in table 1) show negligible charge transfer between MgO and Ag. The bond populations across the interface (between Ag atoms and ions of the perfect MgO(100) substrate) are practically zero. We note that the existence of a good fit of the interfacial energy versus interface distance [14] to the so-called *universal binding energy relation* (similar to the potential energy curve for diatomic molecules) does not necessarily imply chemisorption between metal and substrate (see more in [16]).

Table 1. Energies, distances and charge distribution parameters of the perfect and defective Ag/MgO(100) interfaces. Note that the shell model [17] has ten Ag layers atop 31 MgO planes; for the image interaction model [20] of NiO, the optimum vacancy site is in the second oxide layer.

Ag atom over	Coverage and model	Distance $l^{(0)}$ (Å)	Binding E_b (eV)	Charge[a] $e(00)_{Ag}$ (e)	Dipole $d(10)_{Ag}$ (ea_0)	Quadrupole $q(20)_{Ag}$ (ea_0^2)
Perfect interface						
O^{2-}	1/4 layer	2.58	0.23	0.063	0.251	−0.433
	3 layers	2.43	0.46	0.053[b]	0.418[b]	−1.971[b]
ion	SM [17]	2.60	0.11	—	—	—
	IIM [20]	2.53	0.30	—	—	—
Mg^{2+}	1/4 layer	2.89	0.22	0.038	−0.170	0.414
	3 layers	3.23	0.07	0.042	0.116	−0.686
ion	SM [17]	3.20	0.02	—	—	—
	IIM [20]	2.74	0.60	—	—	—
Defective interface						
F_s centre	1/4 layer	1.83[c]	7.59	0.95(0.92)[d]	−1.61(-0.71)[d]	4.17(0.26)[d]
O	SM [17]	0.5	2.54	—	—	—
vacancy	IIM [20]		2.0	—	—	—
V_s	1/4 layer	0.31[c]	12.67	−1.46(0.09)[d]	0.74(0.16)[d]	0.45(0.2)[d]
centre	cluster [9b]	0.39	11.97	−1.53	—	—

[a] A positive sign means an excess of *electron* density as compared to a neutral Ag atom.
[b] For the interfacial silver layer.
[c] The distance between the Ag atom and the centre of the vacancy.
[d] The numbers in parentheses are the multipoles of ghost orbitals centred on the vacancy.

There is significant redistribution of charge *within* the metal; bond populations between nearest Ag atoms within metal planes parallel to the interface are typically 0.1 e per atom, and are not sensitive to the adsorption site. The concentration of Ag electron density at the *bridge position* between nearest metal atoms has been confirmed in inelastic He scattering studies [34]: only by introducing negative pseudo-charges in these positions in metal films could a good fit be found for theoretical surface phonon-dispersion curves to experimental data. The effective atomic charges and their definitions are discussed further in [35]. Bond population analysis for the three-layer Ag on MgO(100) shows why Ag adsorption over O^{2-} ions is favoured. This stems from electrostatic attraction with enhanced electron density near the hollow position in the interfacial Ag layer (0.07 e from table 1). The extra charge has an attractive interaction with the substrate Mg^{2+} ion below it. For the Ag adsorption over the Mg^{2+} ions, there is instead a repulsion between the electron density localized between Ag atoms, and the substrate O^{2-} ion below it.

The atomic dipole moments ($d(10)$ in table 1) characterize a shift of electron density along the z axis. As expected from the IIM, the dipoles have opposite signs above O and above Mg: metal electrons are repelled by the anion and attracted by the cation. For an Ag monolayer, the dipole moment is largest for Ag over the (optimal) O site. Quadrupole moments ($q(20)$ in table 1) also characterize the deformation, and are affected significantly by Ag 4d–5s orbital

mixing. The negative $q(20)_{Ag}$ found for thicker layers means an axial Ag contraction in the z direction or expansion in the xy plane. The Ag atoms adsorbed on MgO(100) surfaces are considerably deformed. This deformation is the origin of much of the adhesion, and its trends with numbers of Ag layers underlie trends in adhesion energies for defect-free surfaces [16]. Partial (1:4) Ag coverage of the MgO(100) surface shows differences from three-layer (1:1) coverages. For the low (1:4) coverage there is negligible interatomic electron density concentration between Ag atoms; the interatomic charge density is too small to play a role. For Ag adsorption over O^{2-} or Mg^{2+} ions, there is a single nearest substrate ion (either O^{2-} or Mg^{2+}) and four next-nearest substrate ions of the opposite type (either Mg^{2+} or O^{2-}). Adsorption energies for these two cases are close, suggesting compensation of electrostatic attraction and repulsion between the slightly charged Ag adatoms and substrate ions.

For the 1:4 surface coverage, the small charge transfer (0.06 e) from the substrate to each isolated Ag atom is almost the same for three Ag layers atop MgO, but the value of the dipole moment is larger for the thicker Ag layer. The isolated Ag atom charge density is deformed along the z axis, as expected in the IM model. The difference in quadrupole deformation (table 1) may be come from mismatch of Ag and MgO lattice spacings, which has a bigger effect at full coverage. Difference electron density maps, analysed by Zhukovskii *et al* (1999) [16] for low Ag coverage, show that Ag atoms are more polarized above O^{2-} substrate ions. Charge transfer from the substrate is still very small, and it is not clear that chemical bonding is a major factor. The main effects seem to be intra-ionic polarization of Ag and oxide ions. Second neighbours are important, as seen on comparing the effects on MgO(100) and (110) (Zhukovskii *et al* 1999 [16]). The effect is even more pronounced for Ag on the O-terminated α-Al$_2$O$_3$(0001) surface (Zhukovskii *et al* 1998 [16]). Our estimates of the basis-set-superposition error (BSSE) [36] show it to be very small, e.g. for Ag above O^{2-} it is only 0.03 eV.

3.2. Surface defects

The results of defect calculations for low (1:4) Ag coverage are summarized in table 1. We first optimized the geometry of a (bare) pure MgO(100) slab around the neutral F_s^0 and V_s^0 centres, as well as around empty (charged) Mg^{2+} or O^{2-} vacancies. When a ghost orbital was included in the O^{2-} vacancy, its population was 1.72 e, typical of F^0 centres in ionic oxides. The remaining 0.28 e is distributed over two spheres of nearest ions. The F^0 centre thus mimics the O^{2-} ion which it replaces, and there is negligible atomic relaxation of the surrounding ions. Its energy level lies 4.2 eV above the top of the valence band. If we neglect ghost orbitals, the O^{2-} vacancy becomes doubly charged, with the two electrons distributed on nearest-neighbour ions. Four surface Mg^{2+} ions are repelled from the vacancy and shift outwards by 0.16 Å; the axial subsurface Mg^{2+} ion is displaced downwards by 0.23 Å. In the V_s^0 centre calculations the effect of the ghost orbitals is small, since no electron density can be localized inside the Mg^{2+} vacancy. The O^{2-} ions surrounding the Mg^{2+} vacancy shift outwards from the vacancy: four equivalent surface O^{2-} ions move outwards by 0.12 Å, and the axial subsurface O^{2-} ion moves downwards by 0.16 Å. The four surface O^{2-} ions share 1.8 of two holes associated with the V_s^0 centre. This agrees with HF cluster calculations (Ferrari and Pacchioni 1995 [9]).

In the further interface calculations with Ag present, we re-optimized atomic relaxations continuously for every position of an adsorbed Ag atom over the vacancies at which ghost orbitals are centred. When an Ag atom approaches the V_s^0 centre, it donates two of its valence electrons to the four O^{2-} ions surrounding the Mg vacancy. These fill the two holes localized on the O^- ions of the free V_s^0 centre, thus returning the effective charges of these four O^{2-} ions to their values on a pure MgO surface. (The silver effective charge in table 1 is smaller

than $+2\,e$ by 0.5 e due to partial electron delocalization and weak bonding with these O^{2-} ions.) This Ag^{2+} ion substitutes almost perfectly for the Mg^{2+} host ion removed, being only 0.31 Å above the surface plane. This agrees with the conclusions of two previous HF cluster calculations for Cu and Ag on MgO(100) [8, 9]. Large dipole and quadrupole moments, and the difference electron density maps in figure 2(a), indicate that the Ag^{2+} ion is quite strongly polarized and deformed (cf similar data for Ag atom adsorption on the perfect surface given in table 1). The binding energy is very high, 12.67 eV, again agreeing well with a cluster calculation [9]; this is due to a *very* large electrostatic stabilization effect. We use Born–Haber cycles in section 4 to understand the electron transfers between Ag and the neutral metal and neutral oxygen vacancies.

For the Ag atom adsorption over F_s^0 centres, we observe an opposite effect: one electron is transferred from the surface defect to the Ag atom. This results in a pair of opposite charges, Ag^-/F_s^+, with the mutual separation of 1.83 Å, much smaller than for the Ag atom above O^{2-} on a regular surface. The population 0.5 e of the $Ag^- - F_s^+$ bond is quite considerable, whereas all other bonds have negligible populations. The optimized lattice relaxation includes 0.06 Å outward on-plane displacements of Mg^{2+} from the F_s centre, and 0.08 Å vertical displacement of the Mg^{2+} in the plane below the F_s centre. The considerable binding energy can again be supported by electrostatic estimates for the interaction between Ag^- with nearest surface ions. Large dipole and quadrupole moments indicate that Ag^- is contracted and strongly deformed as is also seen from figure 2(b). IIM calculations [20] give the interaction energy between the doubly charged vacancy (preferentially in the subsurface plane) and a *neutral* Ag atom to be ≈ 2 eV which addresses a quite different situation. The latter estimate is close to an atomistic SM prediction of 2.54 eV [17] which also neglects charge transfer.

We also performed calculations for an Ag *monolayer* over an array of the F_s centres in the same concentration (1:4). The binding energy per 2×2 extended unit cell increases by 0.75 eV, i.e. there is an additive effect in the interaction of four Ag atoms with the defect and three regular O^{2-} ions. The adhesion energy for each of the three Ag atoms is $0.75/3 = 0.25$ eV, which is very close to that for a perfect surface with monolayer coverage [16]. The quadrupole moments of Ag atoms in the monolayer are large, which demonstrates their deformation. It is likely that such a monolayer is unstable against faceting.

In any periodic boundary calculation, there is inevitably some band width (energy dispersion) associated with even highly localized defect states. When such 'band' states are only partly occupied, there is some argument for saying the system is conducting. Any real system will have features which inhibit long-range transport, such as the stress and electric fields of random defects, or perhaps special correlation or polaron effects beyond those already included. According to our CRYSTAL calculations, both the perfect MgO(100) slab and the MgO(100) slab with F-centres (for 1/4 surface coverage) are insulating. As to the MgO(100) slab with V-centres (for the same 1/4 coverage), our calculations do suggest it may be conducting. Whether real MgO surfaces with these Mg defects would conduct is an open question, and the few experimental data give no guidance. Both the perfect and defective Ag/MgO(100) slabs are conducting, even for 1/4 Ag coverage; it is probably not surprising that Ag has this effect, even at 1/4 coverage.

4. Charge transfer processes

Our calculations have shown at least three cases in which electrons are transferred to or from the Ag. These are the transfer of an electron from the F_s^0 centre to Ag, the transfer of two electrons from Ag to the V_s^0 centre, and the loss of two electrons by Ag^0 to form Ag^{2+} when it moves into a surface Mg vacancy. The electron transfers have emerged from full electronic
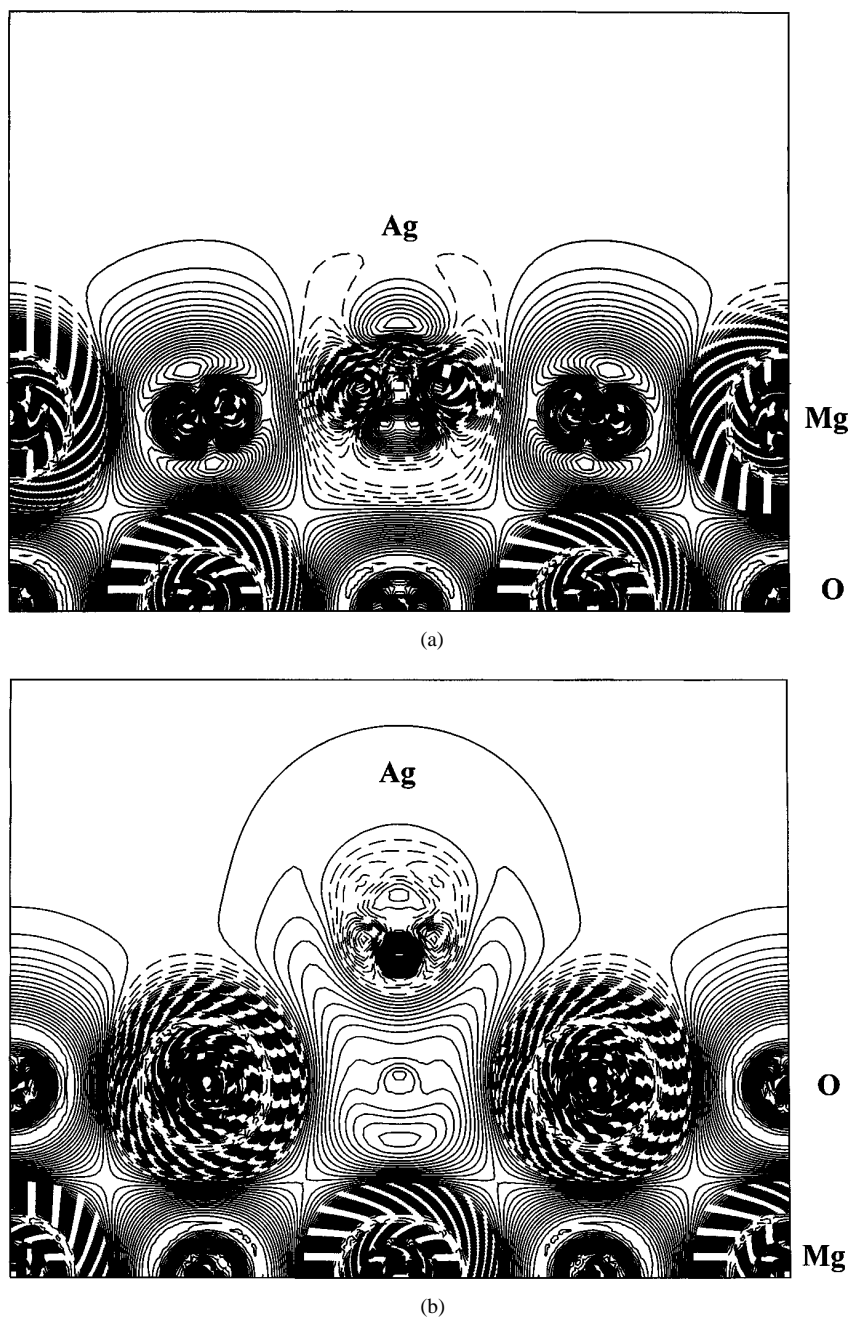
(a)

(b)

Figure 2. The *difference* electron density maps (total density minus superposition of atomic densities) for the cross-section perpendicular to the (100) interface plane for 1:4 Ag adsorption: (a) over a surface V_s centre, showing effectively an Ag^{2+} substituting for Mg^{2+} and (b) over a surface F_s centre, showing noticeable Ag^{-}–F_s^{+} bonding. Isodensity curves are drawn from -1 to $+1$ $e\,a_0^{-3}$ with an increment of $0.0025\,e\,a_0^{-3}$.

structure calculations. We now show that much simpler, less accurate, calculations lead to the same results. The simpler analysis is important because the main energy contributions

are more transparent. Such simpler approaches can be used to identify trends over a range of materials, or to discuss complex systems, or to generalize to other metals.

We shall assume that the Ag behaves like bulk Ag, with a work function of 4.4 eV, i.e. that the Fermi level ε_F is 4.4 eV below vacuum. We now discuss energies which we write in forms such as $\varepsilon(0/+)$. An electron with this energy could be added to the '+' state of the centre considered to form the neutral state without absorbing or releasing energy (for a fuller discussion, see [37]). The important question is whether a particular energy, like $\varepsilon(0/+)$, lies above or below the Ag Fermi level. If it lies above, the '+' state will be stable, i.e. the neutral centre will transfer an electron to the Ag. We now estimate some of the energies relevant for the charge transfers predicted in our full calculations. We emphasize that there may be significant uncertainties (perhaps 1 eV) in the rough estimates. Figure 3 shows the important energy levels schematically.

4.1. Electrons from the surface F_s^0 centre to Ag

Here we use the results of Ferrari and Pacchioni (1996) [9], corrected for some missing but substantial polarization energy terms [38]. These results show:

F_s^0 goes to $F_s^+ + e$ (free) costs 4.2 eV, so $\varepsilon_{Fc}(+/0) = -4.2$ eV
F_s^+ goes to $F_s^{2+} + e$ (free) costs 5.5 eV, so $\varepsilon_{Fs}(2+/+) = -5.5$ eV

The neutral F^0 centre should transfer an electron to the Ag; the remaining electron in the F^+ centre should not transfer. This agrees with our full-scale calculations.

4.2. Electrons from Ag to the surface V_s^0 centre

Again we use the results of Ferrari and Pacchioni (1996) [9] as corrected in [38]

V_s^0 captures free electron costs 7.8 eV, so $\varepsilon_{Vc}(0/-) = -7.8$ eV
V_s^- captures free electron costs 5.9 eV, so $\varepsilon_{Vs}(-/2-) = -5.9$ eV.

In both cases, we expect electrons to be transferred from Ag to the cation vacancy, i.e. we expect the V_s^{2-} state to be obtained. This again agrees with our full-scale calculations.

4.3. Substitutional Ag in an Mg vacancy

Here we ask first of all which charge states of substitutional Ag will be stable at an Mg site in bulk MgO. This type of question was addressed in [37] and [39]. These authors showed in their ionic shell model description that the main terms in the energy are the Madelung energy, the polarization energies and the free ion ionization potentials. There is also a need to know the electron affinity of MgO. Experimentally, this is very uncertain. The results of [39] and [40] showed that the known stable states of transition metal ion dopants in MgO could all be predicted correctly, along with their optical ionization spectra, with a negative electron affinity. Values in the range -1 eV to -3 eV were acceptable. We shall choose -1.0 eV, since this ensures that the known stable charge states of the bulk cation and anion vacancies are also correctly predicted. This value is consistent with known V-centre ionization energies and with estimates from MIES spectra (A L Shluger and V Kempter, private communication). In [37] reasons are discussed for differences between this negative value and certain measurements. The ionization potentials for Ag are similar to the corresponding transition metal values (the first three Ag ionization potentials in eV are 7.57, 21.48 and 34.82) [41]. Following [37] and [39] we find for Ag_{Mg} the values:

$$\varepsilon(0/+) = -1.6 \text{ eV} \qquad \varepsilon(+/2+) = -3.5 \text{ eV} \qquad \varepsilon(2+/3+) = -4.8 \text{ eV}.$$
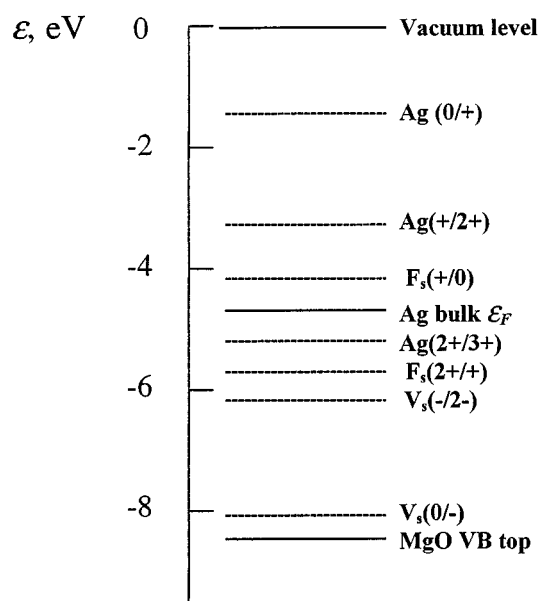
Figure 3. Schematic positions of the basic energy levels ε_i for defects, for Ag and for MgO crystal bands.

The accuracy of these values is not high. For a surface defect, there will be other terms in the energy as well; these terms are of both signs. Nevertheless, if we ask what we should expect if these (bulk) energies do apply for the Ag atom at a surface Mg^{2+} site, we see that the '2+' state is to be expected. This agrees with the conclusions of our full-scale calculations.

There are three comments we should make. First, the simple energies are relatively close and not very accurate. In particular, relatively modest changes in metal work function could lead to changes in what is expected: the '3+' charge state of Ag might be stabilized, or the F_s^0 centre might retain both its electrons. Secondly, there may be other defects which can change charge state. This was addressed in [42] for Ag/NiO. In such cases, the space charge must be treated properly. Thirdly, there is an opportunity to control adhesion by controlling charge states. This we shall address in a separate paper.

5. Conclusions

One important general conclusion to be drawn from our *ab initio* Hartree–Fock calculations is that chemical bond formation is not important for the perfect Ag/MgO(100) interface. This is true also for Ag/MgO(110) (Zhukovskii *et al* 1999 [16]). Physical adhesion associated with polarization and charge redistribution is dominant. The adhesion energy is enhanced by the interaction of the substrate ions with the extra electron density near the interatomic positions of the interfacial Ag layer. This favours silver atoms placed above either surface O^{2-} ions. The difference in predicted optimal Ag adsorption sites observed for this microscopic work and the image model stems mainly from the different treatments of long-range dispersion (van der Waals) interactions. However, these two kinds of calculation complement each other, since they address different situations: the atomistic modelling focuses on several metal planes whereas the image model prediction is for a thick metal layer atop an oxide substrate.

We have also shown here that even neutral surface defects can play a crucial role in metal adsorption kinetics on oxide surfaces and in the adhesion energy of metals to oxides. This is

supported by experimental studies [18, 43, 44]. We find, in full agreement with previous HF cluster calculations [8, 9], an Ag atom placed above a V_s centre donates two of its valence electrons to the four O atoms surrounding the Mg vacancy, transforming into an Ag^{2+} ion, which then is drawn towards the surface and, in effect, substitutes for the missing Mg^{2+} ion. The relevant binding energy is very high, about 12 eV, since there is a very large electrostatic stabilization effect.

In contrast, we also find that Ag atoms atop F_s^0 centres attract one of the defect electrons to form a complex Ag^-/F_s^+ of oppositely charged defects. Here, unlike Ag on the perfect surfaces, there is considerable covalent bonding, which localizes an additional $0.5\,e$. The binding energy is 7.6 eV. Similar HF cluster calculations (Ferrari and Pacchioni 1996 [9]) do not find this effect for a neutral F_s^0 centres but only for the charged F_s^+ centres. The discrepancy could arise from interaction between F_s centres (in our work, the concentration is high), different F_s centre basis sets or the cluster model boundary effects (unlike us, Ferrari and Pacchioni (1996) [9] find Ag atoms bound neither to O^{2-} nor Mg^{2+} on a perfect MgO surface, although Ag^+ ions are bound to O^{2-}, as one would expect).

One important result of our work is the validation of the ideas ([20], Stoneham and Tasker 1985 [25]) that charged defects can enhance adhesion. This was one of the main ideas developed in the image interaction model (Stoneham and Tasker 1985 [25]), although the early papers were not able to exploit full electronic structure methods to handle defects which we discuss here.

Acknowledgments

References

[1] Heinrich V E and Cox P A 1994 *The Surface Science of Metal Oxides* (Cambridge: Cambridge University Press)
[2] Stoneham A M and Tasker P W 1985 *J. Phys.: Condens. Matter* **18** 543
  Stoneham A M 1981 *J. Am. Ceram. Soc.* **64** 64
[3] Finnis M W 1996 *J. Phys.: Condens. Matter* **8** 5811
[4] Ernst F 1995 *Mater. Sci. Eng.* R **14** 97
  Campbell C T 1997 *Surf. Sci. Rep.* **27** 1
  Renaud G 1998 *Surf. Sci. Rep.* **32** 1
[5] Ertl G and Freund H-J 1999 *Phys. Today* No 1 32
[6] *Proc. 4th Int. Symp. on Atomically Controlled Surfaces and Interfaces* 1998 *Appl. Surf. Sci.* **130–132**
  Stoneham A M, Harding J H and Harker A H 1996 *MRS Bull.* **21** 29
[7] Stoneham A M 1983 *Appl. Surf. Sci.* **14** 249
[8] Bacalis N C and Kunz A B 1985 *Phys. Rev.* B **32** 4857
[9] Ferrari A M and Pacchioni G 1995 *J. Phys. Chem.* **99** 17 010
  Ferrari A M and Pacchioni G 1996 *J. Phys. Chem.* **100** 9032
[10] Stoneham A M and Harding J H 1998 *Acta Metall. Mater.* **46** 1155
[11] Schönberger U, Andersen O K and Methfessel M 1992 *Acta Metall. Mater.* **40** S1
[12] Goniakowski J 1998 *Phys. Rev.* B **57** 1935
  Goniakowski J 1998 *Phys. Rev.* B **58** 1189
[13] Li C, Wu R, Freeman A J and Fu C L 1993 *Phys. Rev.* B **48** 8317
[14] Hong T, Smith J R and Srolovitz D J 1994 *J. Adhesion Sci. Technol.* **8** 837
  Hong T, Smith J R and Srolovitz D J 1995 *Acta Metall. Mater.* **43** 2721

[15] Pacchioni G and Rösch N 1996 *J. Chem. Phys.* **104** 7329
      Yudanov I V, Vent S, Neyman K, Pacchioni G and Rösch N 1997 *Chem. Phys. Lett.* **275** 245
      Matveev A V, Neyman K, Pacchioni G and Rösch N 1999 *Chem. Phys. Lett.* **299** 603
[16] Heifets E, Zhukovskii Yu F, Kotomin E A and Causá M 1998 *Chem. Phys. Lett.* **283** 395
      Zhukovskii Yu F, Alfredsson M, Hermansson K, Heifets E and Kotomin E A 1998 *Nucl. Instrum. Methods* **141** 73
      Zhukovskii Yu F, Kotomin E A, Jacobs P W M, Stoneham A M and Harding J H 1999 *Surf. Sci.* **441** 373
[17] Purton J, Parker S C and Bullett D W 1997 *J. Phys.: Condens. Matter* **9** 5709
[18] Duffy D M, Harding J H and Stoneham A M 1995 *Acta Metall. Mater.* **43** 1559
[19] Trampert A, Ernst E, Flynn C P, Fischmeister H F and Rühle M 1992 *Acta Metall. Mater.* **40** S 227
      Guenard P, Renaud G, Vilette B, Yang M-H and Flynn C P 1994 *Scr. Metall. Mater.* **31** 1221
[20] Duffy D M, Harding J H and Stoneham A M 1994 *J. Appl. Phys.* **76** 2791
[21] Schaffner M-H, Patthey F and Schneider W-D 1998 *Surf. Sci.* **417** 159
[22] Harada T, Asano M and Mizutani Y 1992 *J. Cryst. Growth* **116** 243
      Didier F and Jupille J 1994 *Surf. Sci.* **307–309** 587
[23] Duffy D M, Harding J H and Stoneham A M 1996 *Acta Metall. Mater.* **44** 3293
[24] Harding J H, Stoneham A M and Venables J A 1998 *Phys. Rev.* B **57** 6715
[25] Stoneham A M and Tasker P W 1986 *Ceramic Microstructures '86: Role of Interfaces* ed J A Pask (New York: Plenum) p 155
      Stoneham A M and Tasker P W 1985 *J. Phys. C: Solid State Phys.* **18** L543
[26] Dovesi R, Saunders V R, Roetti C, Causá M, Harrison N M, Orlando R and Aprá E 1996 *CRYSTAL-95 User Manual* (Turin: University of Turin)
[27] Causá M and Zupan A 1994 *Chem. Phys. Lett.* **220** 145
[28] Perdew J P and Wang Y 1992 *Phys. Rev.* B **45** 13 244
[29] Causá M, Dovesi R, Pisani C and Roetti C 1986 *Surf. Sci.* **175** 551
[30] Hay P J and Wadt W R 1985 *J. Chem. Phys.* **82** 284
[31] Aprá E, Stefanovich E V, Dovesi R and Roetti C 1991 *Chem. Phys. Lett.* **186** 329
[32] Guenard P, Renaud G and Villette B 1996 *Physica* B **221** 205
[33] Duffy D M, Harding J H, and Stoneham A M (appendix by J R Willis) 1993 *Phil. Mag.* A **67** 865
[34] Kaden C, Ruggerone P, Toennies J P, Zhang G and Benedek G 1992 *Phys. Rev.* B **46** 13 509
[35] Causá M, Kotomin E A, Pisani C and Roetti C 1987 *J. Phys. C: Solid State Phys.* **20** 4391
[36] Grimes R W, Catlow C R A and Stoneham A M 1989 *J. Phys.: Condens. Matter* **1** 7367
[37] Stoneham A M and Ramos M M D 1993 *J. Solid State Chem.* **106** 2
[38] Stoneham A M and Harding J H 1999 *Ceramics into the 2000s Part C: Proc. 1998 World Ceramic Congr., CIMTEC*
[39] Stoneham A M and Sangster M J L 1980 *Phil. Mag.* B **43** 609
[40] Sangster M J L, Stoneham A M and Tasker P W 1981 *Phil. Mag.* B **44** 603
[41] Moore G E 1971 *Atomic Energy Levels (Ser. Natl Bur. Stand. US 35)* vol 1 (Washington, DC: US Government Printing Office)
[42] Duffy D M, Harding J H and Stoneham A M 1995 *J. Appl. Phys.* **76** 2791
[43] He J-W and Møller P J 1986 *Chem. Phys. Lett.* **129** 13
      He J-W and Møller P J 1986 *Surf. Sci.* **178** 934
      He J-W and Møller P J 1987 *Surf. Sci.* **180** 934
      Astrup I and Møller P J 1988 *Appl. Surf. Sci.* **33/34** 143
[44] Meunier M and Henry C R 1994 *Surf. Sci.* **307** 514